

Effects of Common Sterilization Methods on the Structure and Properties of Poly(D,L Lactic-Co-Glycolic Acid) Scaffolds

HOLLY SHEARER, M.Eng., MARIANNE J. ELLIS, Ph.D., SEMALI P. PERERA, Ph.D.,
and JULIAN B. CHAUDHURI, Ph.D.

ABSTRACT

While methods for the production of scaffolds with the appropriate mechanical properties and architecture for tissue engineering are attracting much attention, the effects of subsequent sterilization processes on the scaffold properties have often been overlooked. This study sought to determine the effects of sterilization with ethanol, peracetic acid, ultraviolet irradiation, and antibiotic solution on the structure of 50:50 (mol:mol) 65:35, and 85:15 poly(D,L-lactic-co-glycolic acid [PLGA]) flat-sheet and hollow-fiber scaffolds. All methods resulted in scaffold sterilization, but scanning electron microscopy revealed deformations to the scaffold surface for all treatments. The extent of surface damage increased with treatment duration. This was further investigated by measurement of pore sizes, water flux, breaking strain, and Young's modulus. External pore size and water flux was found to be increased by all treatments in the following order: ethanol (largest), antibiotics, ultraviolet light, and peracetic acid. Pore sizes were 0.25 to 0.17 μm and water flux ranged from 0.01 $\text{kg} \cdot \text{m}^{-2} \cdot \text{s}^{-1}$ to 3.34 $\text{kg} \cdot \text{m}^{-2} \cdot \text{s}^{-1}$. For all samples, the Young's modulus was 1.0 to 31.1 MPa and breaking strain was 1.2 to 2.4 MPa. The results of this study suggest that antibiotic treatment shows the most potential to sterilize PLGA hollow fibers for tissue engineering.

INTRODUCTION

TISSUE ENGINEERING IS WIDELY ANTICIPATED TO REPLACE traditional graft procedures for treatment of tissue and organ defects. Successful tissue generation *in vitro* requires highly specialized scaffolds. Mass transfer, topography,¹ surface chemistry,^{1,2} mechanical properties,³ and degradation rates³ are just some of the factors that influence the ability of cells to colonize a scaffold, produce extracellular matrix molecules, and form an organized tissue construct. Implantation *in vivo* requires the scaffold to be biocompatible, integrate with the surrounding natural tissue, and, in many situations over a favorable time scale, to be completely eliminated from the host via biodegradation.

Materials and production methods for suitable polymer scaffolds attract much research attention; however, the effects of sterilizing these scaffolds before cell seeding are often overlooked. Low polymer melting points, complex

architectures, and hydrolytic degradation mechanisms result in scaffolds that may be easily damaged by harsh sterilization protocols. Typical medical or cell culture sterilization methods may prove unsuitable for polymer scaffolds. For example, standard techniques such as autoclaving, ethylene oxide treatment, or gamma irradiation have been shown to be unsuitable for polymer scaffolds because of deformation from elevated temperatures, lengthy degassing, and deterioration due to decreased molecular weights.⁴

This study investigates 4 methods for sterilizing flat-sheet and hollow-fiber poly(D,L-lactic-co-glycolic) (PLGA) scaffolds with the objective of achieving scaffold sterilization with minimal or no structural damage. The treatments comprise 70% ethanol treatment; ultraviolet irradiation; peracetic acid treatment; and antibiotic treatment with penicillin G, streptomycin sulfate, and amphotericin B. Changes to the topography of the scaffold, which may affect the ability of cells to adhere to the scaffold, were determined by

scanning electron microscopy. Gas permeation and water flux were measured to calculate the effects of sterilization method on the pore diameter and to quantify mass transfer parameters, respectively. The mechanical properties of the fiber were determined by measuring the breaking stress and strain.

MATERIALS AND METHODS

Preparation of polymer flat sheets and hollow fibers

Polymer solutions were prepared from 50:50 (mol:mol), 65:35, and 85:15 PLGA (Alkermes, Inc., Cincinnati, Ohio) with 1-methyl-2-pyrrolidinone (NMP; Acros Organics, Geel, Belgium) in a 20% (w/w) solution.⁵ Flat-sheet scaffolds were formed by solvent exchange with distilled water; 100- μm thickness sheets were cast onto glass supports and immersed in distilled water at 10–15°C. After a few minutes the scaffolds were lifted off the glass support but left in water for 24 h to ensure solvent removal. The scaffolds were then removed from the water tank and dried in ambient conditions (8–20°C) for at least 24 h. The 50:50 PLGA hollow fibers were wet-spun through a double-orifice spinneret; polymer was extruded under low pressure (approximately 2 barg) through the outer annular orifice (outer diameter, 1.0 mm; inner diameter, 0.7 mm), polymer flow rate was controlled with a ball valve. Distilled water was filtered (40 μm ; Swagelok, Bristol, UK) and pumped concurrently through the inner orifice (inner diameter, 0.4 mm) at a rate of 3.5–7.0 mL min⁻¹. Fibers passed through 2 water tanks, and a motorized roller guided them at a rate of 7–9 m min⁻¹ into a final water tank, where they were left for 24 h before drying in ambient conditions (8–20°C).

Sterilization treatment

Flat sheets were cut into circular 13-mm (outer diameter) membrane supports (Minucells and Minutissue, Vertriebs GmbH, Bad Abbach, Germany), excess scaffold was removed with a scalpel. Hollow fibers were cut into 10-mm lengths. One flat-sheet or 2 hollow-fiber sections were sterilized in individual cells in a polystyrene 24-well plate (Nunclon, Nalge Nunc International, Roskilde, Denmark). Both flat-sheet and hollow-fiber samples had a mean mass of 4 ± 0.6 mg (mean \pm SD; $n = 12$) before treatment.

Ethanol sterilization. A 1 mL 70% (v/v) ethanol solution (diluted from 96% [v/v] ethanol [Fisher Scientific UK Ltd, Loughborough, UK], with distilled water) was added to each sample. Samples were treated for 15 min, 30 min, 1 h, 2 h, 5 h, and 24 h and were subsequently rinsed 5 times with 1 mL phosphate-buffered saline (PBS; Sigma-Aldrich, Dorset, UK).⁶ For water flux experiments, fibers were treated after potting into the bioreactor by submerging the

reactor in ethanol solution for 30 min, followed by rinsing thoroughly with deionized water.

Ultraviolet treatment. Irradiation was carried out with a 12-W ultraviolet lamp (Syngene, Cambridge, UK) at 254-nm wavelength at a distance of 15 cm. Samples were irradiated for a total time of 30 min, 1 h, 2 h, and 5 h,⁷ and were turned over halfway through the treatment to irradiate the top and bottom surfaces. Flat-sheet samples were also prepared without turning.

Antibiotic treatment. Polymer samples were placed in a solution of 1% (v/v) antibiotic antimycotic solution (10 000 units mL⁻¹ penicillin G, 10 mg mL⁻¹ streptomycin sulfate, and 25 $\mu\text{g mL}^{-1}$ amphotericin B [Sigma-Aldrich, Dorset, UK] in PBS and incubated at 4°C for 6 h, 15 h, 24 h, and 31 h. Samples were rinsed 3 times with PBS before use.

Peracetic acid treatment. Peracetic acid treatment was performed for the same time intervals as for ethanol treatment with a solution of 0.1% (v/v) peracetic acid (peracetic acid solution 39% in acetic acid, Sigma-Aldrich, Gillingham, UK), 4% (v/v) ethanol 95.9% (v/v) distilled water. Samples were rinsed 3 times in 1 mL PBS for 1 h each.⁸

Preparation of controls. Control flat-sheet samples were prepared as for antibiotic treatment; PBS or distilled water replaced the antibiotic solution. Samples were not rinsed after treatment. Untreated control scaffolds were also tested.

Analysis

Sterility testing. 50:50 PLGA samples were incubated for 48 h at 37°C and 5% carbon dioxide in 1 mL media (Dulbecco's modified Eagle's medium [GIBCO, Paisley, UK], supplemented with 10% fetal bovine serum, 1% nonessential amino acids [Sigma-Aldrich, Dorset, UK], and 1% sodium pyruvate [GIBCO]) and checked periodically for signs of infection, indicated by yellowing of the media (Dulbecco's modified Eagle's medium contains the indicator phenol red) and increased media opacity. Unsterilized scaffolds were used as a positive control, and media with no scaffold was used as a negative control.

Scanning electron microscopy. Samples were prepared with a scalpel to reveal all the surfaces; liquid nitrogen was used as required to freeze the polymer and prevent structural damage. Samples were mounted on a sample tray using double-sided sticky carbon discs and sputtered with gold (5150B sputter coater, BOC Edwards, West Sussex, UK) before being viewed with the scanning electron microscope (JSM6310, JEOL, Herts, UK). The surface porosity and pore size were approximated from scanning electron microscopy images using ImageJ software.⁹ Pore size and porosity could be estimated only for samples showing a high contrast between the pores and the polymer surface.

Measurements could not be made for highly wrinkled surfaces.

Gas permeation. Hollow fibers 120 mm long were sterilized in batches of 12 in 70-mL glass boiling tubes. The membrane characterization technique of gas permeation was used to determine pore diameter. Samples were glued using epoxy resin (Araldite Rapid, Huntsman, Everberg, Belgium) into 10-cm-long, 6-mm-diameter stainless-steel tubes. At one end the lumen of the fiber was sealed, and at the other end space around the fiber (the ablumen) was sealed. Nitrogen permeation through the fiber walls was measured for inlet pressures between 1 barg and membrane failure (typically 5–6 barg). Pore sizes were calculated on the basis of the assumption of Poiseuille flow through porous media; permeation flux was plotted against transmembrane pressure, allowing the intercept (K_0) and gradient (P_0) to be used with the gas constant (R), the temperature (T), the molecular weight of the gas (M), and the gas viscosity (μ) to calculate pore radius (r).¹⁰

$$r = \frac{16}{3} \left(\frac{P_0}{K_0} \right) \left(\frac{8RT}{\pi M} \right)^{0.5} \mu \quad (1)$$

Water flux. Samples were prepared as for gas permeation and fitted into a stainless-steel custom bioreactor; a 100-mm-long, 12-mm-diameter tube formed the body of the reactor with two 6-mm side ports. Ten fibers were placed in the bioreactor; the shell side was sealed at both ends using epoxy resin. Water circulated through the tube side by means of a peristaltic pump (503U, Watson-Marlow Bredel Pumps Ltd, Cornwall, UK); permeate was collected on the shell side. Pressure gauges (0–6 barg; Bailey & Mackey Ltd., Birmingham, UK) measured inlet and outlet pressures, and a nonrotating stem valve on the outlet controlled the transmembrane pressure.

Mechanical testing. Hollow fibers were tested to breaking tension (model 1122 electromechanical test system, Instron, Norwood, MA) with a full scale load of 500 g and a cross-head speed of 20 mm min⁻¹. Samples were tested dry or were kept in distilled water after sterilization and tested within 30 min. Ultraviolet and control wet samples were soaked in distilled water for 2 h before testing. Breaking stress (σ) and Young's modulus (E) were calculated as follows:

$$\sigma = \frac{mg}{A} \quad (2)$$

$$\varepsilon = \frac{l}{L} \quad (3)$$

$$E = \frac{\sigma}{\varepsilon}, \quad (4)$$

where m is load at failure, g is acceleration due to gravity, A is fiber cross-sectional area, ε is strain, l is extension, and L is original length.

Statistics

A 2-tailed Student's t -test was performed to assess statistical differences between treated samples and the control and between wet and dry samples for the mechanical properties. Statistical difference was defined as $p < .05$ for a 95% confidence interval.

RESULTS

Scaffold structure

Flat-sheet and hollow-fiber scaffolds were successfully fabricated from 20% (w/w) PLGA in 1-methyl-2-pyrrolidinone solution. Scanning electron microscopy analysis revealed that flat sheets had an asymmetric cross-section, with a dense skin (1–2 μ m thick) present on the top, below which a region of parallel pores ran perpendicular to the surface; the bottom of the sheet exhibited a random pore network with large macropores (Fig. 1). Hollow-fiber cross-sections showed skin layers approximately 8–10 μ m on the interior and exterior of the fiber (Fig. 1). Parallel finger-like pores extended halfway across the fiber wall from both the interior and exterior of the fiber.

Effect of sterilization on scaffold structure

Sterilization effectiveness was determined qualitatively by the absence of signs of infection after a 48-h culture period; infection was indicated by a change of indicator color and opacity of culture medium. Only the 50:50 polymer composition was tested for sterilization effectiveness because no difference in the ability of the 4 sterilization treatments to sterilize different PLGA ratios was anticipated. Two hollow-fiber and 2 flat-sheet samples were tested for each combination of treatment and duration. Unsterilized controls all showed infection, and all control media (i.e., no scaffold) remained free of infection for the time period. All the treated scaffold samples indicated successful sterilization in treatment durations equal to or less than those quoted in literature (Table 1).^{6–8} These results indicate the suitability of the sterilization technique to the particular scaffolds. While the full treatment duration suggested in the literature was not always found to be required, it is assumed that the low stringency of the sterility assay could not justify a reduction in treatment duration. Treatment duration for sterilization was therefore assumed to be 30 min for ethanol, 2 h for ultraviolet light and peracetic acid, and 24 h for antibiotic antimycotic treatment. The structure of the scaffolds changed over the complete treatment range; in all cases increasing the treatment duration led to an increased effect on the structure.

Table 2 gives details of the scanning electron microscopy images of all the scaffolds both before and after sterilization treatment, along with estimates of porosity and pore size from ImageJ.⁹ The scanning electronic microscopy

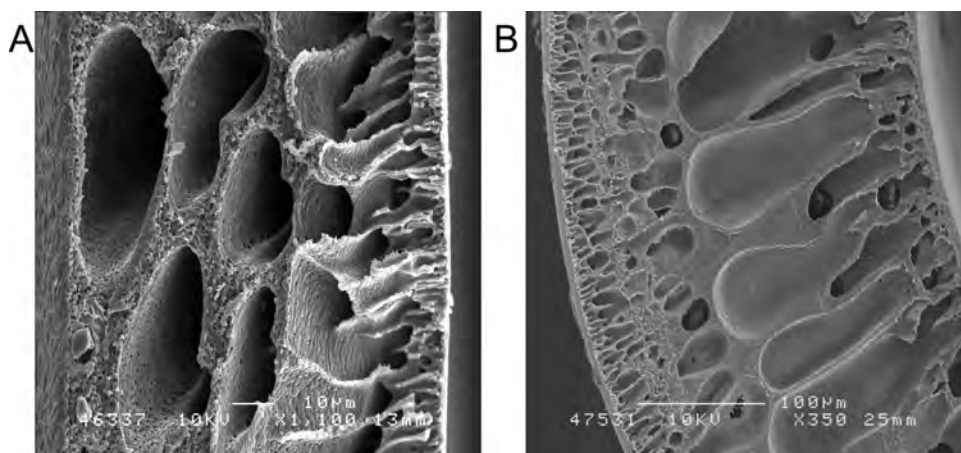


FIG. 1. Cross-section views of poly(D,L-lactic-co-glycolic acid) flat-sheet and hollow-fiber scaffolds illustrating the presence of skin on the top of the flat sheet and both interior and exterior of the hollow fiber. (A) Flat sheet with 1–2- μm skin on the top surface. (Scale bar, 10 μm .) (B) Hollow fiber with 8–10- μm skin on both surfaces. (Scale bar, 100 μm .)

images of the 50:50 PLGA flat sheets and hollow fibers are shown in Figs. 2 and 4, respectively. The scanning electron microscopy images of the untreated control samples all showed homogeneity across the top surfaces; pore sizes for all 3 polymer compositions were similar, with the 65:35 sample showing a slightly lower porosity. The bottom surface of the flat sheets appeared more irregular, with larger pores confined to patches of localized increased porosity. Pores appeared larger on the hollow fibers than on the flat surfaces, and the exterior of the fiber appeared rougher than the interior, with wrinkles and lines of pores following the length of the fiber.

Samples sterilized in ethanol showed reduced porosity on the top surface of the flat sheet and increased surface wrinkling (Fig. 2D). The porous patches on the bottom of the flat sheets appeared more prominent, with larger pores following longer treatment durations (Figs. 2C and 3).

Hollow fibers exhibited larger pores on the interior of the fiber (Fig. 4C), while the exterior of the fiber (Fig. 4D) showed very few pores after treatment. After less than 10 min in ethanol, the longer hollow fibers had deformed and fused together (Fig. 5). The membranes treated with ethanol for longer periods were more fragile under scanning electron microscopy; magnifications above $\times 2500$ resulted in damage to the sample within seconds.

Ultraviolet-treated scaffolds showed little change in porosity (Fig. 2E and F). The exterior of the fibers showed smoothing of the surface and smaller pores (Fig. 4F). The interiors of hollow fibers were not directly exposed to ultraviolet light and consequently showed very little change in appearance (Fig. 4E).

Peracetic acid had a large impact on the surface of the scaffolds as compared to the controls (Fig. 2G and H and Fig. 4G and H). Surfaces appeared much more

TABLE 1. COMPARISON OF TREATMENT METHOD AND DURATION REQUIRED FOR STERILIZATION OF FLAT-SHEET AND HOLLOW-FIBER POLY(D,L-LACTIC-CO-GLYCOLIC ACID) SCAFFOLDS*

Treatment	Time									
	0	0.25 h	0.5 h	1 h	2 h	5 h	6 h	15 h	24 h	31 h
Negative control (no sample)	√	—	—	—	—	—	—	—	—	—
Positive control (not sterilized)	×	—	—	—	—	—	—	—	—	—
Ethanol	×	×	√	√	√	—	—	—	√	—
Ultraviolet light (turned)	×	—	×	√	√	√	—	—	—	—
Ultraviolet light (not turned)	×	—	×	√	√	√	—	—	—	—
Peracetic acid	×	√	√	√	√	—	—	—	√	—
Antibiotics	×	—	—	—	—	—	√	√	√	√

*Two hollow-fiber and 2 flat-sheet samples were tested for each combination of treatment and duration. Unsterilized controls showed signs of infection in the time period; all control media (no scaffold) showed no signs of infection for the time period. √ indicates no sign of infection after 48 h of culture in Dulbecco's modified Eagle's medium with 10% fetal calf serum, 1% nonessential amino acids, 1% sodium pyruvate at 37°C 5% carbon dioxide, × indicates infection may have occurred in some or all samples (media changed from pink to yellow and became opaque). Dashes indicate that treatment/duration combination was not tested. Shading indicates that times were equal to or longer than duration required for sterilization quoted in literature.^{5–9}

TABLE 2. COMPARISON OF EFFECT OF FOUR METHODS OF STERILIZATION ON THREE POLYMER COMPOSITIONS AND TWO SCAFFOLD FORMS*

<i>Scaffold</i>	<i>Control</i>	<i>30-min Ethanol</i>	<i>2-h Ultraviolet light</i>	<i>2-h Peracetic acid</i>	<i>24-h Antibiotics</i>
50:50 PLGA flat sheet					
Top	Slightly wrinkled with an even distribution of pores Porosity ~ 10% Pore diameter ~ 0.5 μm	Surface shows increased wrinkling Porosity ~ 1% Pore diameter ~ 0.4 μm	Pores slightly smaller and rounder than control Porosity ~ 9% Pore diameter ~ 0.4 μm	Large variation in pore size; cracks in surface Porosity ~ 8% Pore diameter ~ 0.4 μm	Wrinkled surface Decreased porosity and pore size
Bottom	Smooth with some irregular patches about 50–100 μm diameter showing increased porosity; very few pores outside these regions Pores much larger in than top surface	Very patchy, with all pores within porous regions ~ 50–100 μm in diameter Pores are larger than in upper surface	Porous patches with reduced number of larger pores	Many porous regions with large pores	Greater number of porous regions with larger pores than control
65:35 PLGA flat sheet					
Top	Smooth with well-defined pores Porosity, 7% Pore diameter, 0.4 μm	Wrinkled with very few pores Porosity ~ 0% Pore diameter, 0.4 μm	Increased porosity Porosity ~ 12% Pore diameter ~ 0.5 μm	Wrinkled with cracks along troughs Pore diameter ~ 0.4 μm	Smooth with large pores Porosity ~ 17% Pore diameter ~ 0.6 μm
Bottom	Regions showing increased porosity and cracking are elongated, ~ 25 μm wide and 100–150 μm long Surface wrinkling present	Circular patches < 50 μm diameter showing increased porosity	Circular patches with ~ 25 μm of increased porosity	Surface is wrinkled, with porous regions	Smooth with even distribution of pores
85:15 PLGA flat sheet					
Top	Smooth with even distribution of pores Porosity ~ 11% Pore diameter ~ 0.4 μm	Very few pores, surface wrinkling Porosity ~ 4% Pore diameter ~ 0.4 μm	Slightly wrinkled with evenly distributed pores Porosity ~ 11% Pore diameter ~ 0.4 μm	Wrinkled surface, large range of pore sizes with some cracks Pore diameter ~ 0.2 μm	Large pores showing regions of increased porosity Porosity, 13% Pore diameter, 0.7 μm
Bottom	Larger pores with some irregular regions showing increased porosity	Patches of increased porosity	Large range of pore sizes, patches with larger pores, small pores all over surface	Regions of increased porosity	Large pores and cracks visible in surface
50:50 hollow fiber					
Inside	Large variation in pore size	Highly porous	Pores aligned along length of fiber	Large cracks	Very porous and uneven surface
Outside	Even distribution of pores, grooves aligned with fiber	Few pores	Fewer pores than inside, aligned along length of fiber	Small pores and surface wrinkling along length of fiber	Small pores and irregular surface wrinkling

*PLGA: poly(D,L-lactic-co-glycolic acid).

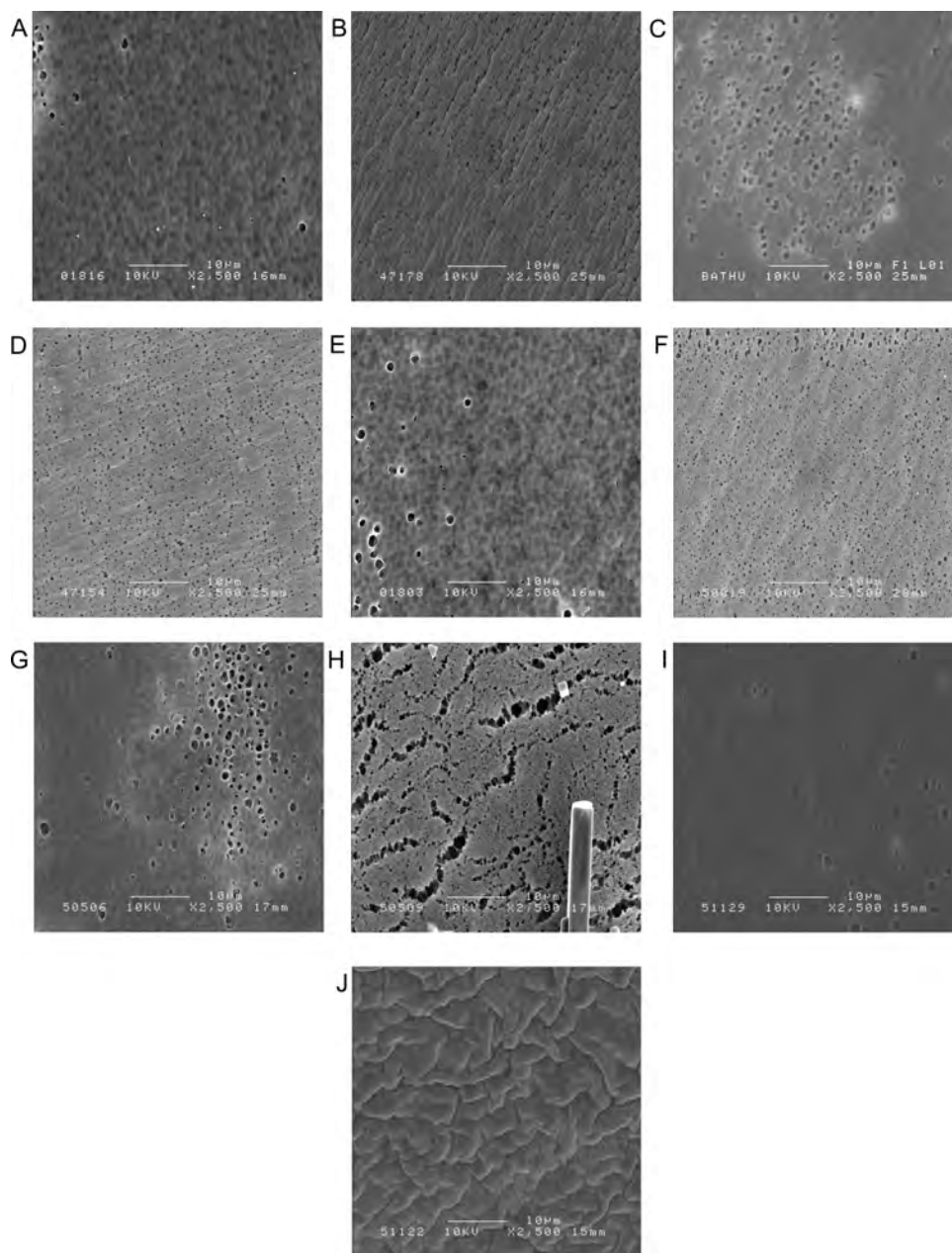


FIG. 2. Surfaces of poly(D,L-lactic-co-glycolic acid) flat sheet following sterilization treatment. (Scale bar, 10 μm .) (A) Bottom of control sample. (B) Top of control sample. (C) Bottom of ethanol-treated sample. (D) Top of ethanol-treated sample. (E) Bottom of ultraviolet-treated sample. (F) Top of ultraviolet-treated sample. (G) Bottom of peracetic acid-treated sample. (H) Top of peracetic acid-treated sample. (I) Bottom of antibiotic-treated sample. (J) Top of antibiotic-treated sample.

wrinkled, with cracks and large pores. Salt crystals were also observed, which may have been a result of interactions between the acid and PBS used to rinse the scaffolds. PBS was used to rinse other samples with no adverse effects. The increased surface wrinkling and salt crystals prevented the determination of porosity with ImageJ.

A high degree of damage was associated with antibiotic treatment compared to the controls. Increased surface wrinkling was present on all surfaces, with a high density

of small pores on the top of the flat sheets (Fig. 2J). The bottom of the flat sheets showed significantly fewer, larger pores (Fig. 2I). The skin layer appeared to have completely dissolved on the interior of the hollow fibers (Fig. 4J). The outer surface of the fibers showed increased wrinkling with fewer pores (Fig. 4I).

Some change in polymer structure was observed for control samples treated with water or PBS, but to a lesser degree than the sterilized samples.

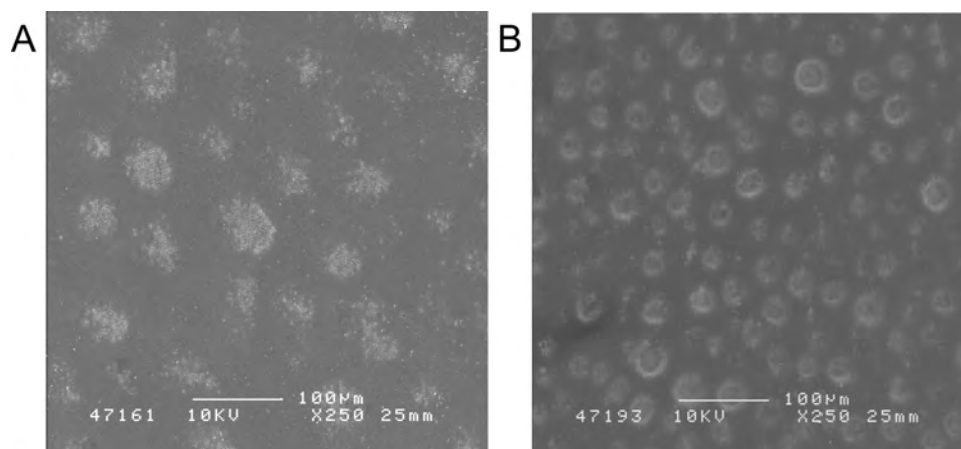


FIG. 3. Bottom surface (as formed and treated) of poly(D,L-lactic-co-glycolic acid) flat sheet following treatment with 70% (v/v) ethanol. (Scale bar, 100 μm .) (A) Treated for 30 min. (B) Treated for 2 h.

Scanning electron microscopy images revealed that all 3 polymer compositions responded to the sterilization treatment in a similar manner. Therefore, further tests on gas permeation, water flux, and mechanical testing were carried out only on the 50:50 polymer ratio.

Characterization of sterilized scaffolds by gas permeation, water flux, and mechanical stress measurements

All sterilization treatments resulted in an increased external skin pore diameter as indicated by gas permeation. Pore size for the samples was in the following order (largest to smallest): ethanol, antibiotic, ultraviolet light, peracetic acid, and control; however, the differences were not statistically significant (Fig. 6). The ethanol sample exhibited a large SD; this is thought to be due to the extent of damage caused by ethanol treatment and irregularities in the fiber resulting from the spinning process (Fig. 7). All treated samples exhibited higher water fluxes than the control (Fig. 8), with the same order as with gas permeation. The largest water flux, the ethanol sample, was 55 times larger than that of the control.

Mechanical testing revealed a significant ($p < .05$; $n = 3$ samples from same batch of fibers) reduction in breaking stress for the dry ethanol sample (1.21 MPa) against both the dry control (2.42 MPa) and the wet ethanol sample (1.57 MPa) (Fig. 9). Significant differences in Young's modulus were also found between the wet (18.2 MPa) and dry (31.1 MPa) control, and the wet (11.1 MPa) and dry (27.2 MPa) ethanol samples, with dry samples exhibiting higher Young's moduli. There was also a significant reduction in Young's modulus for the dry ultraviolet light sample compared with the control. The peracetic acid and antibiotic samples showed little change in breaking stress compared to the control and an insignificant reduction in Young's modulus.

DISCUSSION

Sterilization treatments were investigated to find an effective method for sterilizing PLGA structures, without damaging the scaffold, for use as *in vitro* scaffolds for tissue engineering. All sterilization treatments reduced the chances of the sample becoming infected under culture conditions; however, structural damage was evident in all cases. While the assay used to determine sterilization cannot be considered conclusive with regard to the possibility of incomplete sterilization not being indicated over the 48-h culture period, the results are supported by other studies.^{7,11,12}

Ethanol at concentrations of 60–80% (v/v) is classified as a disinfectant, rather than a sterilization agent, because of its inability to destroy hydrophilic viruses or bacterial spores;¹¹ however, ease of use and apparent effectiveness make ethanol a favorable, and widely used, tool for *in vitro* studies.

This study found that ultraviolet sterilization was achieved within 1–2 h. This finding is supported by other studies in the literature showing that treatment for 2 h results in complete sterilization of the sample. Our concern with the use of ultraviolet sterilization is its ability to sterilize larger 3-dimensional scaffolds throughout (e.g., the porous hollow fibers). However, we found that there was no need to turn either scaffold form in order to achieve sterilization; this finding suggests that ultraviolet radiation, with sufficient intensity for sterilization, can pass through thin polymer membranes. However, the sterilization of larger, thicker scaffolds would need to be assessed separately.

The U.S. Food and Drug Administration has approved peracetic acid for sterilizing tissues such as skin or bone.¹² Our results suggest that treatment of just 15 min was sufficient to sterilize; however, protocols in the literature suggest a duration of 2–3 h.^{8,12}

To our knowledge, the published literature contains no reports on pretreatment with antibiotics for sterilization.

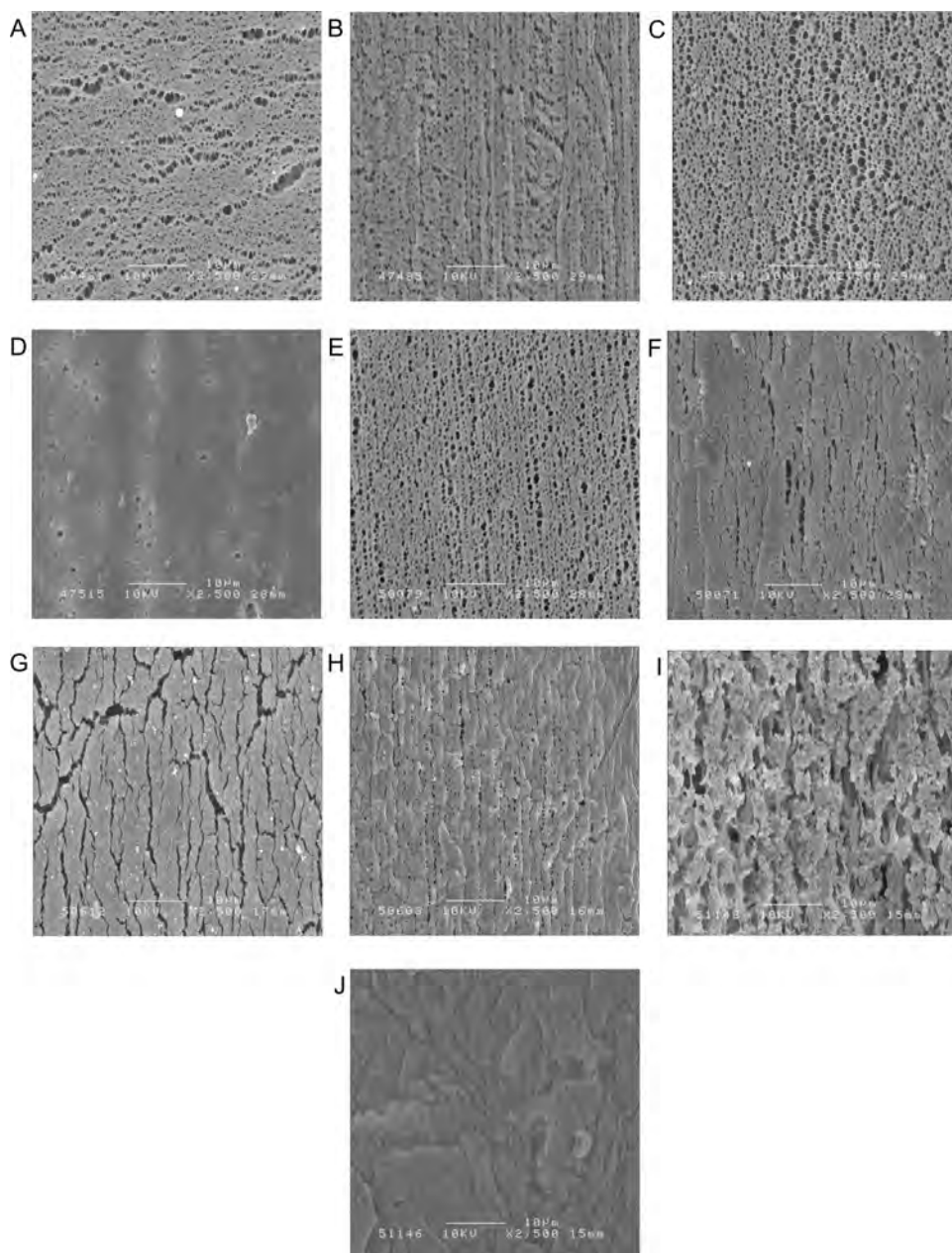


FIG. 4. Surfaces of poly(D,L-lactic-co-glycolic acid) hollow fiber following sterilization treatment. (Scale bar, 10 μm .) (A) Inside of control sample. (B) Outside of control sample. (C) Inside of ethanol-treated sample. (D) Outside of ethanol-treated sample. (E) Inside of ultraviolet-treated sample. (F) Outside of ultraviolet-treated sample. (G) Inside of peracetic acid-treated sample. (H) Outside of peracetic acid-treated sample. (I) Inside of antibiotic-treated sample. (J) Outside of antibiotic-treated sample.

Antibiotic treatments were therefore performed over a wide range of treatment durations. Our results indicate that sterilization was achieved after the shortest test duration (6 h). However, because of the low stringency of the assay, we adhered to recommendations of 24-h treatment.

While all polymer surfaces showed structural variations resulting from processing, the observed trends of damage increasing with sterilization duration suggest the damage resulting from specific treatments. Scaffold surfaces were categorized into 3 groups according to their surface struc-

ture: flat sheet upper surface with a thin skin layer (1–2 μm) above a section of parallel pores perpendicular to the surface; flat sheet lower surface with macro pores, and surfaces of the hollow fibers with thicker skin layers (8–10 μm) and parallel pores perpendicular to the surface. Rapid exchange of solvent with water at the edges of the scaffold during fabrication leads to fast contraction of the polymer chains, forming dense skins.¹³ Scanning electron microscopy consistently revealed greater damage by sterilization to the bottom of the flat sheets, suggesting that the

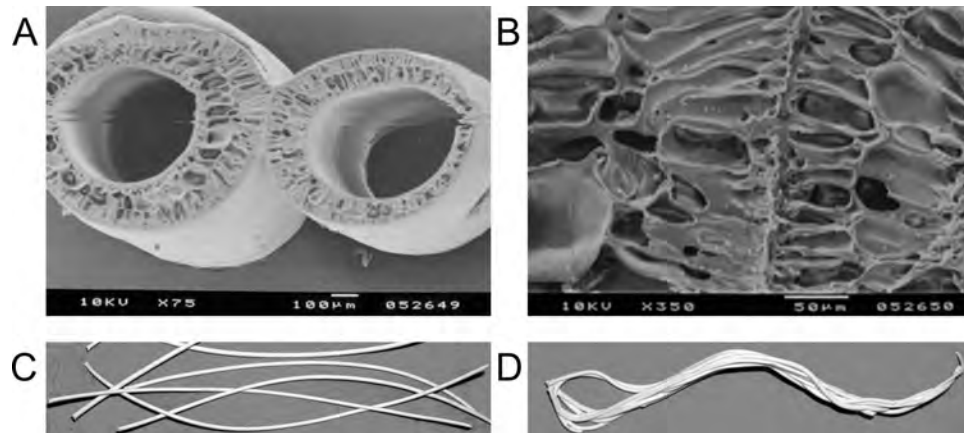


FIG. 5. (A and B) Scanning electron microscopy image of fibers fused together—(A) original magnification, $\times 75$; scale bar, $100\ \mu\text{m}$; (B) original magnification, $\times 350$; scale bar, $50\ \mu\text{m}$. (C) 120-mm-long fibers before ethanol treatment. (D) 120-mm-long fibers fused together after ethanol treatment for 30 min.

presence of skin protects the scaffold from the harmful effects of sterilization. Patches of increased porosity on the bottom of the flat sheets would be consistent with a large macro void adjacent to the surface. Any removal of polymer from this surface would result in the exposure of more of these void regions, resulting in more and larger porous patches. Similar removal of polymer on the other membrane surfaces would not break through the skin, resulting in little change to the appearance of the scaffold.

Damage caused by ethanol treatment was unexpected. Reports of similar processes in literature make no comment of structural damage,⁶ and ethanol has been reported elsewhere to result in no morphologic or chemical damage to polyester scaffolds.¹¹ The form of the hollow-fiber scaffolds is thought to have highlighted this problem, which may not have been apparent for other scaffold structures. The only indication of ethanol damage on flat sheets was patches of increased local porosity. The membrane support maintained the shape of the flat-sheet scaffolds during treatment, whereas the unsupported nature of the hollow fibers revealed the deformation caused. The membrane

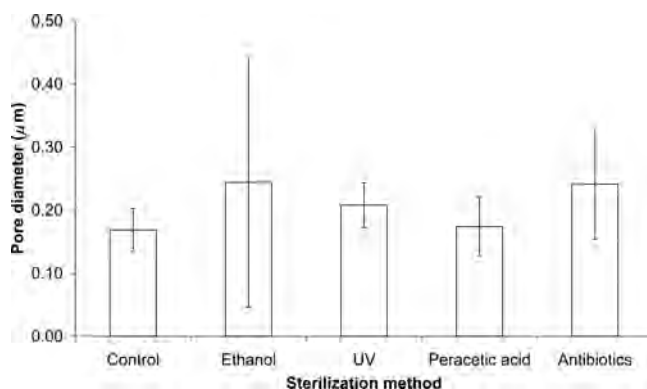


FIG. 6. Average pore diameter of hollow fibers (measured in micrometers) following sterilization treatment, determined via nitrogen gas permeation. UV: ultraviolet.

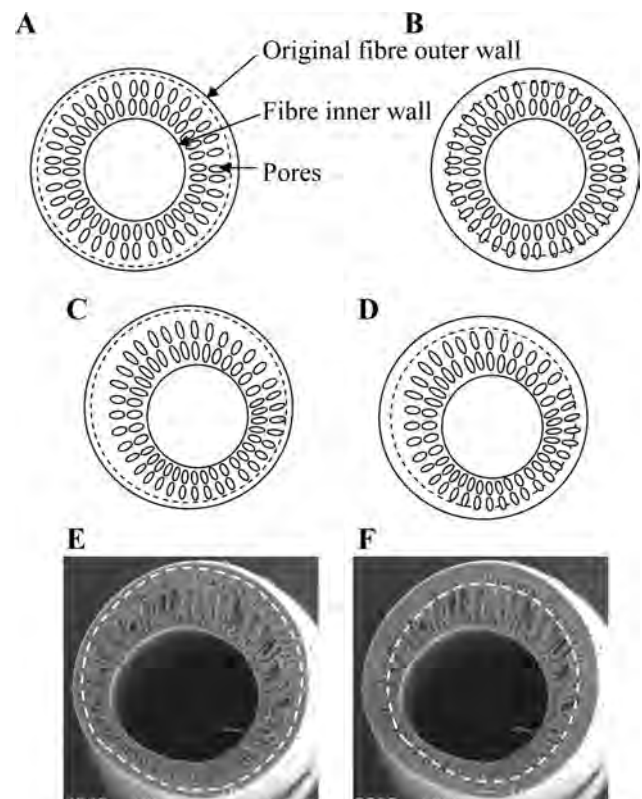


FIG. 7. Small changes in extent of damage to hollow fibers by sterilization treatment can result in large changes in surface pore size, particularly if the fiber is asymmetric. Dotted lines show outer circumference of fiber following treatment. (A) Treatment does not completely remove skin layer; therefore surface porosity changes little. (B) A small increase in extent of damage by treatment results in complete removal of skin layer and a large increase in surface porosity. (C and E) Even with irregular fibers, a small degree of damage by treatment will not penetrate the skin region of the fiber. (D and F) If the fiber is asymmetric as the extent of damage increases, some areas of the porous interior of the fiber will be exposed and some will not, leading to a greater degree of variation in the properties exhibited by the fiber.

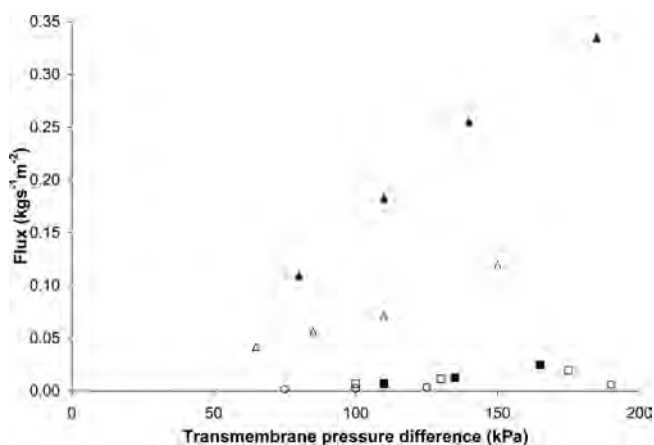


FIG. 8. Average water flux through fiber against transmembrane pressure (control ○; ethanol 30 min ▲; ultraviolet light 2 h ■; peracetic acid 2 h □; antibiotic/antimycotic 24 h △;). Data were collected over a single unit containing 10 fibers for each treatment. Flux values are reported per unit surface area.

characterization techniques revealed the increases in water flux. This reduction in mass transport resistance suggests an opening of internal channels; together with the morphologic changes, this indicates partial dissolution of polymer in ethanol. Subsequent deposition of polymer, driven by high polymer concentrations at the solid-liquid interface, may have caused fusion of fibers treated together.

Ultraviolet treatment had the least impact on the scaffold appearance; all the samples except the 85:15 flat sheet showed a slight decrease in surface roughness. Pore size and porosity showed little change following ultraviolet treatment. The mechanical test revealed a reduction in Young's modulus for the dry sample. A similar investigation into the effects of ultraviolet sterilization on poly(D,L-lactic acid)-poly(ethylene glycol)-monomethyl ether (Me.PEG-PLA)⁷ also found a decrease in surface roughness and polymer molecular weight; however, this was reported to be a result of removal of PEG from the scaffold surface. While this cannot be the reason for the increased smoothness of PLGA, energy provided by ultraviolet light may provide activation energy for similar photo-oxidative reactions and cleavage of ester bonds.

Peracetic acid treatment resulted in increased pore size, increased surface roughness, and cracking. Acidic environments are known to catalyze the degradation of PLGA,¹⁴ so it is likely the changes to the scaffold result from degradation of the polymer. Pores will be opened up and in some cases join together, forming cracks, by the removal of polymer from regions where the polymer is thinnest (at the edge of pores).

Antibiotic treatment was found to increase surface roughness, pore diameter, and water flux, with little change in the mechanical properties of the scaffold.

Changes to the scaffold are not necessarily detrimental; increased pore diameter and water flux increase nutrient

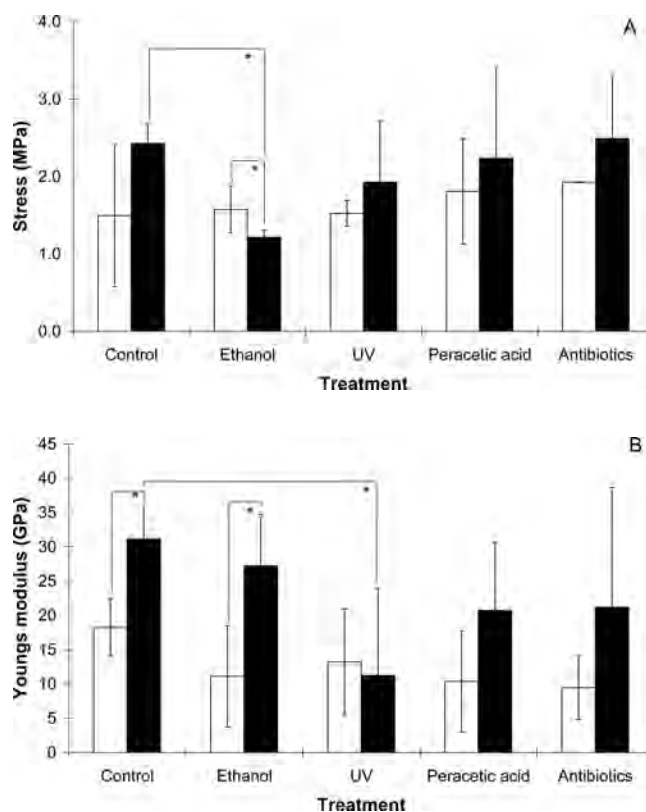


FIG. 9. Average hollow-fiber breaking strain (MPa) (**top**) and Young's modulus (MPa) (**bottom**); 500 g full-scale load, cross-head speed 20 mm min^{-1} ($n = 3$; mean \pm SD; * $p > .05$). Black bars indicate samples that were tested dry; white bars indicate samples that were tested wet.

transfer across the membrane. Pore diameters for the treated samples were $0.15\text{--}0.25 \mu\text{m}$, which relates to a molecular weight cutoff of approximately $1500\text{--}2500 \text{ kDa}$.¹⁵ These values are above the molecular weight cutoff of other hollow-fiber bioreactors,¹⁶ indicating that the pores are large enough for the transport of nutrients across the membrane yet small enough to prevent the ingress of cells into pore entrances. Increased water flux exhibited by the ethanol and antibiotic samples of up to 3.34 and $1.19 \text{ kg m}^{-2} \text{ s}^{-1}$, respectively, over the control value of $0.01 \text{ kg m}^{-2} \text{ s}^{-1}$ may also improve delivery of nutrients to cells.

Knowledge of the effects of sterilization allows incorporation of these effects into scaffold design. Further investigation into the mechanisms of the damage caused, or other sterilization treatments, could yield treatments that do not damage the scaffold. However, the delicate nature and required degradability of tissue-engineering scaffolds means that changes will start to occur as soon as they are formed, which is likely to be accelerated by any treatment. The final selection of sterilization method depends on the scaffold and application in question. The small changes in structure and properties exhibited by the ultraviolet and antibiotic samples will probably have little effect on the suitability of a scaffold for tissue engineering. In particular,

antibiotic treatment provides a simple, reliable sterilization method that is likely to have minimal detrimental effect on the use of a scaffold for tissue engineering.

CONCLUSIONS

This study has shown the significance of the effects of sterilization on PLGA scaffolds. All sterilization techniques successfully reduced the chance of the sample becoming infected. Pore size and water flux were found to increase following all the sterilization treatments, and visible changes to the surfaces were detected via scanning electron microscopy in all cases.

This study has shown that one of the most common sterilization techniques (soaking in 70% ethanol) causes substantial damage to PLGA scaffolds. While the changes caused by ultraviolet light are unlikely to have any detrimental effects on the performance of the scaffolds with respect to tissue engineering, the ability of ultraviolet light to sterilize larger, 3-dimensional scaffolds remains unclear. In addition, the ultraviolet sterilization process requires scaffolds to be treated in a sterile environment before being placed in the bioreactor. A liquid sterilization process eliminates the need to handle the fibers between sterilization and use. Peracetic acid treatment resulted in less structural damage to the scaffold, but the increased irregularity to the surface caused by the presence of cracks may prove detrimental to cell attachment. Antibiotic treatment shows increased pore size, water flux, and surface roughness over the control.

The objective of this study was to determine the most suitable sterilization technique for PLGA hollow-fiber scaffolds. While the results show that none of the sterilization methods are ideal in terms of sterilizing the sample without causing structural changes, it is thought the antibiotic treatment will provide a convenient, effective sterilization method with which to sterilize PLGA hollow fibers for use as a tissue-engineering scaffold.

ACKNOWLEDGMENTS

We gratefully acknowledge the financial support of the Biotechnology and Biological Sciences Research Council. We also thank Hugh Perrott at the Centre for Electron Optical Studies for assistance using the scanning electron microscope and Chris Arnold in the Department for Physics for help with mechanical testing.

REFERENCES

1. Curtis, A.S.G., Gadegaard, N., Dalby, M.J., Riehle, M.O., Wilkinson, C.D. W., and Aithchison, G. Cells react to nanoscale order and symmetry in their surroundings. *IEEE Trans. Nanobioscience* **3**, 61, 2004.
2. Jansen, E.J.P., Sladek, R.E.J., Bahar, H., Yaffe, A., Gijbels, M.J., Kuijjer, R., Bulstra, S.K., Guldemonds, N.A., Binderman, I., and Koole, L.H. Hydrophobicity as a design criterion for polymer scaffolds in bone tissue engineering. *Biomaterials* **26**, 4423, 2005.
3. Hutmacher, D.W. Scaffolds in tissue engineering bone and cartilage. *Biomaterials* **21**, 2529, 2000.
4. Athanasiou, K.A., Niederauer, G.G., and Agrawal, C.M. Sterilisation, toxicity, biocompatibility and clinical applications of polylactic acid/ polyglycolic acid copolymers. *Biomaterials* **17**, 93, 1996.
5. Ellis, M.J. Development of a novel hollow fibre membrane for use as a tissue engineered bone graft scaffold [PhD Dissertation]. Department of Chemical Engineering, University of Bath, Bath, United Kingdom, 2005.
6. Karp, J.M., Shoichet, M.S., and Davies, J.E. Bone formation on two-dimensional poly(DL-lactide-co-glycolide) (PLGA) films and three-dimensional PLGA tissue engineering scaffolds in vitro. *J. Biomed. Mater. Res.* **64A**, 388, 2003.
7. Fischbach, C., Tessmar, J., Lucke, A., Schnell, E., Schmeer, G., Blunk, T., and Gopferich, A. Does UV irradiation affect polymer properties relevant to tissue engineering? *Surf. Sci.* **491**, 333, 2001.
8. McFetridge, P.S., Daniel, J.W., Bodamyali, T., Horrocks, M., and Chaudhuri, J.B. Preparation of porcine carotid arteries for vascular tissue engineering applications. *J. Biomed. Mater. Res.* **70A**, 224, 2004.
9. Rasband, W.S. ImageJ. National Institutes of Health, Bethesda, Maryland, 1997-2004. Accessed August 30, 2006, at <http://rsb.info.nih.gov/ij>.
10. Li, K., Kong, J.F., Wang, D.A., and Teo, W.K. Tailor-made asymmetric PVDF hollow fibers for soluble gas removal. *AICHE J.* **45**, 1211, 1999.
11. Holy, C.E., Cheng, C., Davies, J.E., and Shoichet, M.S. Optimizing the sterilization of PLGA scaffolds for use in tissue engineering. *Biomaterials* **22**, 25, 2001.
12. Huang, Q., Dawson, R.A., Pegg, D.E., Kearney, J.N., and MacNeil, S. Use of peracetic acid to sterilize human donor skin for production of acellular dermal matrices for clinical use. *Wound Repair Regen.* **12**, 276, 2004.
13. Chung, T.-S., and Hu, X. Effect of air-gap distance on the morphology and thermal properties of polyethersulfone hollow fibers. *J. Appl. Polym. Sci.* **66**, 1067, 1997.
14. Middleton, J.C., and Tipton, A.J. Synthetic biodegradable polymers as orthopedic devices. *Biomaterials* **21**, 2335, 2000.
15. Planchamp, C., Vu, T.L., Mayer, J.M., Reist, M., and Testa, B. Hepatocyte hollow-fibre bioreactors: design, set-up, validation and applications. *J. Pharm. Pharmacol.* **55**, 1181, 2003.
16. Kumar, S., Wittmann, C., and Heinzle, E. Minibioreactors. *Biotech Lett.* **26**, 1, 2004.

Address reprint requests to:
Julian. B. Chaudhuri, Ph.D.
Centre for Regenerative Medicine
Department of Chemical Engineering
University of Bath
Bath, United Kingdom

E-mail: cesjbc@bath.ac.uk